A new-concept gamma calorimeter at ELI-NP

2017 JINST 12 C02051

(http://iopscience.iop.org/1748-0221/12/02/C02051)

Published by IOP Publishing for Sissa Medialab
Received: *December 10, 2016*
Accepted: *January 26, 2017*
Published: *February 15, 2017*

14TH Topical Seminar on Innovative Particle and Radiation Detectors
3–6 October 2016
Siena, Italy

A new-concept gamma calorimeter at ELI-NP

M. Lenzi,[a,1] **O. Adriani,**[a,b] **S. Albergo,**[c,d] **M. Andreotti,**[e] **D. Berto,**[f] **R. Borgheresi,**[a,b] **G. Cappello,**[c] **P. Cardarelli,**[e] **R. Ciaranfi,**[a] **E. Consoli,**[e,f] **G. Di Domenico,**[e,f] **F. Evangelisti,**[e] **M. Gambaccini,**[e,f] **G. Graziani,**[a] **M. Marziani,**[e,f] **L. Palumbo,**[g,h] **G. Passaleva,**[a] **M.G. Pellegriti,**[c] **A. Serban,**[a,2] **O. Starodubtsev,**[a] **M. Statera,**[e,f] **A. Tricomi,**[c,d] **A. Variola**[i] **and M. Veltri**[a,j]

[a] *Istituto Nazionale di Fisica Nucleare, Sezione di Firenze, via G. Sansone 1, 50019 Sesto Fiorentino (FI), Italy*
[b] *Dipartimento di Fisica e Astronomia, Università di Firenze, via G. Sansone 1, 50019 Sesto Fiorentino (FI), Italy*
[c] *Istituto Nazionale di Fisica Nucleare, Sezione di Catania, via Santa Sofia 64, 95123 Catania, Italy*
[d] *Dipartimento di Fisica e Astronomia, Università di Catania, via Santa Sofia 64, 95123 Catania, Italy*
[e] *Istituto Nazionale di Fisica Nucleare, Sezione di Ferrara, via Saragat 1, 44122 Ferrara, Italy*
[f] *Dipartimento di Fisica e Scienze della Terra, Università di Ferrara, via Saragat 1, 44122 Ferrara, Italy*
[g] *Istituto Nazionale di Fisica Nucleare, Sezione di Roma, Piazzale A. Moro 2, 00185 Roma, Italy*
[h] *Dipartimento di Scienze di Base e Applicate all'Ingegneria, Università di Roma La Sapienza, Piazzale A. Moro 2, 00185 Roma, Italy*
[i] *Istituto Nazionale di Fisica Nucleare, Laboratori Nazionali di Frascati, via E. Fermi 40, 00044 Frascati (Roma), Italy*
[j] *Dipartimento di Scienze Pure e Applicate, Università di Urbino, Piazza della Repubblica 13, 61029 Urbino, Italy*

E-mail: michela.lenzi@fi.infn.it

Abstract: ELI-NP is an European Research Infrastructure that will provide a monochromatic, high brilliance gamma beam with tunable energy up to 19.5 MeV. The time structure of the beam consists of 32 high intensity gamma bunches separated by a time interval of 16 ns and delivered at a repetition rate of 100 Hz. In order to match such unprecedented beam specifications, specific devices and techniques have been developed to measure and monitor the beam parameters during the commissioning and the operational phase. This paper presents an overview of the gamma beam characterization system, with particular focus on a new-concept sampling calorimeter made of silicon detectors and polyethylene absorbers.

Keywords: Beam-line instrumentation (beam position and profile monitors; beam-intensity monitors; bunch length monitors); Calorimeter methods; Si microstrip and pad detectors

[1] Corresponding author.
[2] On leave from National Institute for Nuclear Physics and Engineering Horia Hulubei, Magurele, Romania.

doi:10.1088/1748-0221/12/02/C02051

2017 JINST 12 C02051

Contents

1 Introduction 1

2 The gamma beam characterization system 2

3 The gamma calorimeter: working principle 3

4 The gamma calorimeter: design 4

5 The gamma calorimeter: readout board 5

6 The gamma calorimeter: test results on a first prototype 7

7 Conclusions 9

1 Introduction

The ELI-NP facility (Extreme Light Infrastructure — Nuclear Physics), currently under construction in Romania, is one of the pillars of the European project ELI and is devoted to the generation of high intensity gamma beams for frontier research in nuclear physics [1, 2]. The ELI-NP gamma beam system will deliver an intense gamma beam with unique characteristics in terms of brilliance, photon flux and energy bandwidth in an energy range from 0.2 to 19.5 MeV. The main parameters of the gamma beam are summarized in table 1. The most efficient process to meet such challenging specifications is the inverse Compton scattering of a laser pulsed at high rate off a high intensity electron beam with energies up to 720 MeV. The energy of the scattered photons is strongly correlated with the scattering angle; an excellent energy bandwidth can therefore be obtained by collimating the beam [3].

A characterization system providing a measurement of the energy spectrum, intensity, space and time profile of the beam is essential for the development and commissioning phase, as well as to monitor the beam stability during operation. The system must be able to cope with pulses of about 10^5 photons with duration of 1-2 ps, and with a pulse-to-pulse time separation of 16 ns. These pulses are packed in macro-pulses, which are bunches of 32 pulses at 100 Hz of repetition rate. The capability of assessing the time dependence of the beam intensity within a macro-pulse, in addition to its long-term stability, is also a strong requirement of the system.

In the next sections, an overview of the whole characterization system is given, followed by a detailed description of a new-concept sampling calorimeter that has been designed with the aim to measure average energy and intensity of the gamma beam.

Table 1. Main parameters of the ELI-NP Gamma Beam System.

	Beam Parameters
Gamma Energy (Eγ)	0.2–19.5 MeV
Energy bandwidth (ΔEγ/Eγ)	$\leqslant$ 0.5%
#Photons/s within bandwidth	up to 8.3×10^8 ph/s
Peak Brilliance	$> 10^{19}$ ph/s$\cdot$ mm$^2\cdot$ mrad^2 0.1% BW

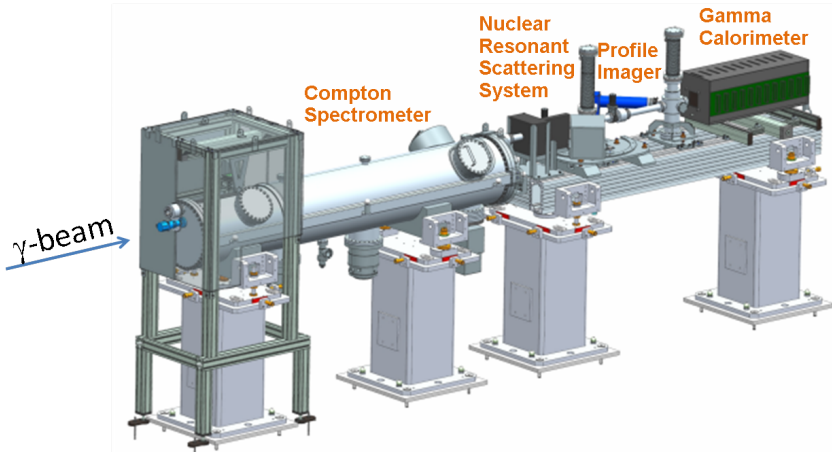

Figure 1. Overview of the gamma beam characterization system.

2 The gamma beam characterization system

In order to match the challenging beam specifications reported in table 1, specific devices and techniques have been developed to measure and monitor the beam parameters. The gamma beam characterization system, shown in figure 1, consists of four detectors, each carrying out different tasks.

The Compton spectrometer is designed to measure the photon energy spectrum and the energy bandwidth; this is achieved by placing an ultra thin target on the beam line and measuring the energy and the angle of the Compton scattered electron. The requirement of time coincidence with the recoil gamma is used for background reduction. In addition, the use of a fast gamma detector allows the pulse originating the Compton interaction to be identified. The energy of the scattered electron is precisely measured by a high purity germanium detector and the scattering angle is determined by a double-sided silicon strip detector. To detect the recoil gamma, Barium Fluoride crystals were chosen. Thanks to the minimal interference with the beam operation, the spectrometer can be operated for continuous beam energy monitoring during the operational phase.

The absolute energy calibration for the other detectors is provided by the Nuclear Resonant System, consisting of a target, made by nuclei that can be excited at properly selected energies, placed on the beam line [4]. When the gamma beam energy overlaps with the energy of a nuclear level of the target, an emission of de-excitation photons takes place. A fine scan of beam energy is performed until the resonant condition is found. Two kinds of crystals are used to detect the re-emitted photons: Barium Fluoride for a fast response, providing prompt information about the

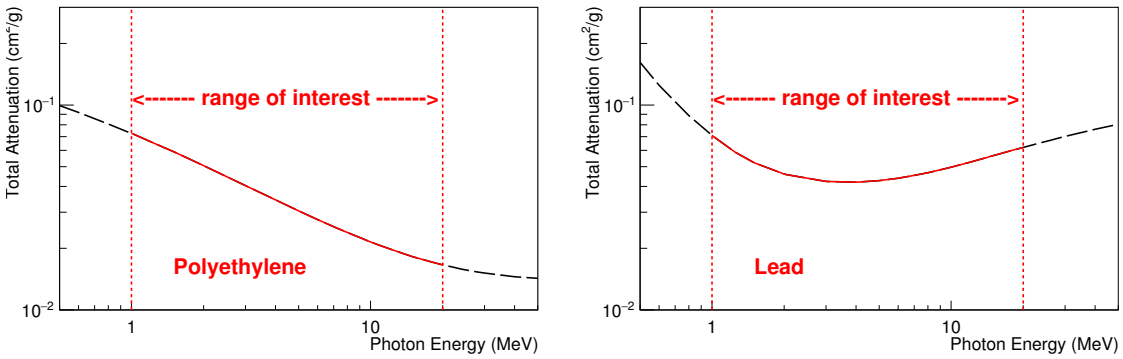

Figure 2. Total photon attenuation as a function of photon energy, in polyethylene and lead materials.

re-emitted gamma counting rate, and LYSO for a precise energy measurement, once the resonant condition is reached.

The Gamma Profile Imager is designed to determine the beam profile, in order to measure the size and the uniformity of the gamma beam. In addition it will be used to check the alignment and operation of the collimation system. The Imager consists of a scintillating target, placed on the beam line, whose emitted light is collected by a CCD camera.

Finally a Gamma Calorimeter will provide the average energy and intensity of the beam. The original approach adopted and the results of the tests done with the first prototype are the subject of this work and will be described in detail in the next sections.

3 The gamma calorimeter: working principle

The very challenging gamma beam characteristics, in particular the short duration of the beam pulse and the unknown number of photons per pulse, prevent the use of traditional gamma spectroscopic techniques. Therefore, in order to evaluate the beam energy and intensity, a specifically designed detector has been developed.

The basic idea consists in exploiting the monotonic energy dependence of the total photon interaction cross section for low-Z materials, in the energy range of interest at the ELI facility. This behaviour is related to the predominance of Compton scattering interactions with respect to pair production. As an example, figure 2 reports the total attenuation coefficient for the low-Z polyethylene (left) and the high-Z lead (right), a material commonly used in calorimeter detectors. Due to this characteristic energy dependence, the average depth of a photon interaction inside a low-Z absorber is expected to increase with energy. In the case of a monochromatic photon beam impinging on a sampling calorimeter with low-Z absorber, the longitudinal profile of the energy deposition can be uniquely related to the photon energy and can be parametrized as a function of the beam energy through detailed Monte Carlo simulations of the device. The average beam energy can therefore be reconstructed by comparing the measured profile against the simulated ones. Once the photon energy is determined, in the hypothesis of a monochromatic beam, the beam intensity can also be inferred from the measured total energy release, after correcting for the expected leakage that is also obtained from simulations. In the case of ELI-NP, this approach takes advantage of

2017 JINST 12 C02051

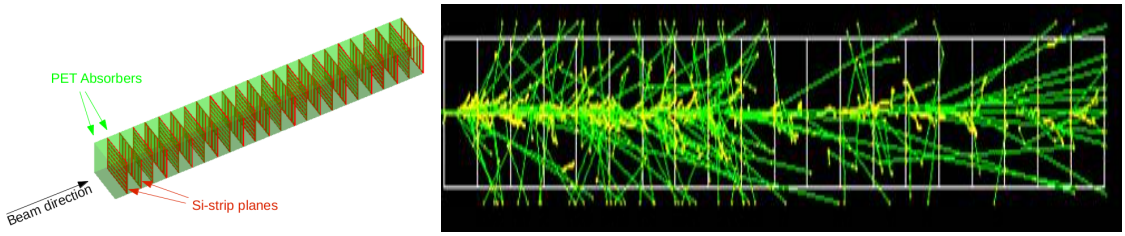

Figure 3. Left: conceptual layout of the calorimeter. Right: an example of a simulated event.

the narrow bandwidth of the beam energy and of the high number of impinging photons, which suppresses the fluctuations of the shower profile.

4 The gamma calorimeter: design

The gamma calorimeter is designed as a sampling device composed of 22 identical layers. Each layer consists of a block of 30 mm of passive absorber made of Polyethylene, an inexpensive and easy to machine low-Z material, followed by a thin silicon detector layer. Silicon technology was chosen for the active layers for its ability to provide a fast response time, allowing us to disentangle the signal due to different pulses within a macro-pulse. It also provides the necessary radiation hardness to survive to the extremely high photon flux and space density of the photons expected at the ELI-NP gamma beam. In addition, silicon detectors meet the required efficiency and response linearity for a wide range of energy deposition values, up to the ones expected at the ELI-NP facility.

The chosen sensors are silicon strip detectors originally developed by Hamamatsu for the CMS experiment [5]. All the sensors are processed from n-type phosphorous doped wafers, 320 μm thick, and are segmented in 128 p^+ strips with 80 μm pitch and 20 μm width. The active area is 10.32×80.00 mm^2. These sensors take profit of the technologies developed in the last 15 years for the LHC tracking systems, leading to radiation hard detectors that can safely sustain irradiation up to 100 kGy. In order to reduce the response time, we plan to operate them at a bias voltage of 600 V. This value, well above the full depletion voltage, guarantees the achievement of the saturation of the charge drift velocity. Since we are not interested in measuring the impact position of the impinging particles, all the strips in each sensor will be wire-bonded together. Each silicon layer is made of seven adjacent silicon sensors. The analog sum of the pulses coming from the seven sensors of the same layer is digitized and readout, as explained in section 5. Such a design allows covering a large active area while keeping the detector capacitance low enough (around 300 pF) to achieve a fast response and an efficient charge collection.

The calorimeter provides a destructive measurement; for this reason it will be installed on a movable platform which will be pulled back during normal beam operations.

The design of the calorimeter has been optimized and validated by means of detailed Geant4 [6] simulations. Figure 3 shows (left) the detector layout reproduced in the simulations and (right) an example of a typical event at ELI-NP. Figure 4 (left) shows the longitudinal shower profile for different beam energies for a single photon pulse of nominal intensity, which corresponds to 10^5 impinging photons. In figure 4 (right) the expected performances are displayed in terms of resolution on the average beam energy and on the number of photons, again for a simulated single pulse. The

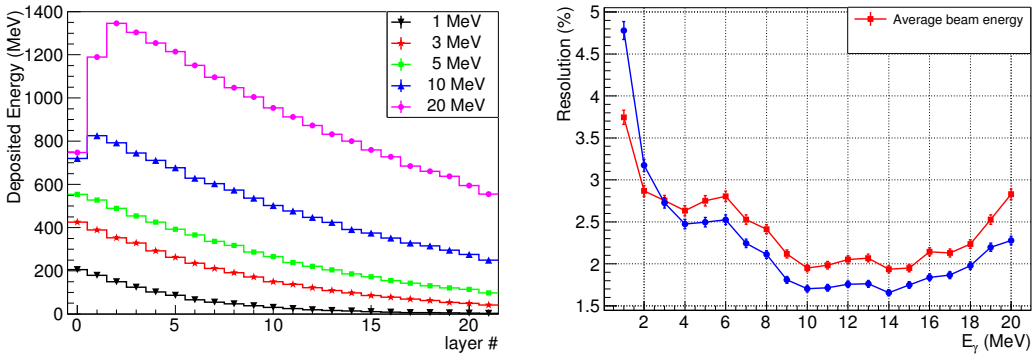

Figure 4. Left: expected energy deposition in each silicon layer for different values of beam energy. Right: expected resolution on the photon energy and the number of photons as a function of the beam energy.

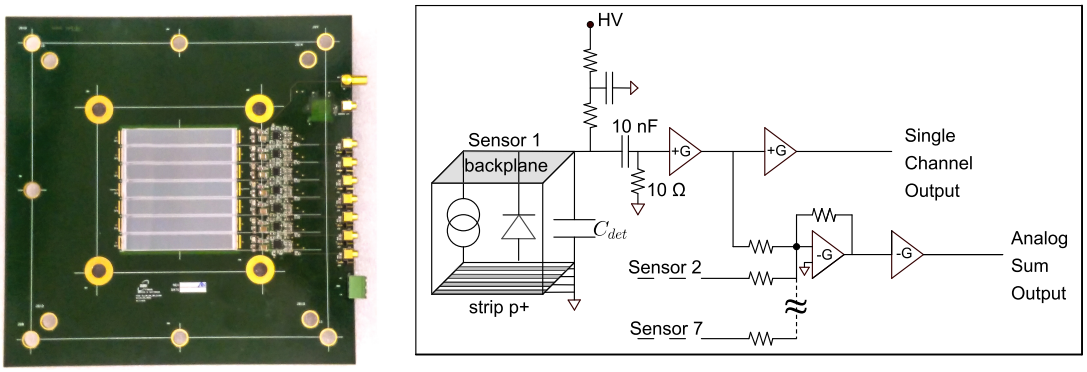

Figure 5. Left: a prototype of the custom readout board equipped with seven silicon devices. Right: schematic diagram of the front-end circuit.

simulated resolutions turn out to be of the order of a few percent, which implies that the statistical accuracy is expected to become better than 1 per mil after a few seconds of operation.

The maximum expected dose on a single silicon sensor for beam energies ranging from 1 to 20 MeV varies in the interval (1.6-8.0)$\times 10^{-4}$ Gy/s. Since the calorimeter will be hold on the beam line only during the commissioning phase, we don't expect a degradation of silicon performances due to irradiation. For this reason we plan to operate the calorimeter at room temperature.

5 The gamma calorimeter: readout board

A custom readout board has been designed in order to comply with the demanding requirements imposed by the ELI-NP gamma beam characteristics, in particular the ability to disentangle pulses separated by 16 ns. The designed readout board provides the front-end electronics for the sensor readout and the mechanical support for the accurate positioning of the sensors in each layer. Figure 5 (left) shows a first prototype of the custom readout board equipped with seven silicon detectors. Figure 5 (right) shows the schematic diagram of the front-end circuit. Each sensor is connected both to an individual readout channel and to an analog sum circuit which will provide the signal

2017 JINST 12 C02051

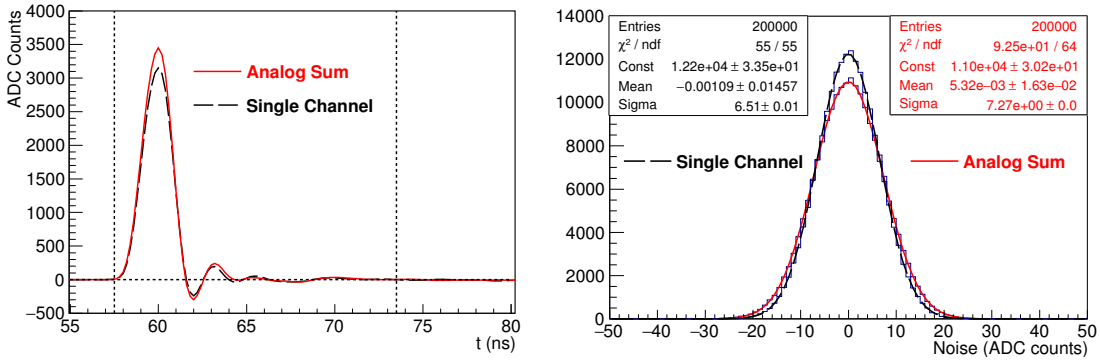

Figure 6. Left: digitized readout signal as a function of time, obtained by injecting a fast (~ 2ns) pulse in the electronics. The vertical dashed lines indicate the 16 ns time separation between two consecutive pulses. Right: sampled electronic noise.

corresponding to the total energy released in the layer. For the first two layers, each sensor will be readout independently, thus providing a rough transverse energy profile, while for the other layers only the sum signal will be digitized for subsequent storage and analysis.

The shape of the signal pulse produced from a single event strongly depends on the input characteristics of the circuit to which the detector is connected, usually a charge preamplifier followed by a shaping amplifier. In order to achieve a very fast signal we decided to avoid the use of a pulse shaper and to integrate the current directly into the amplifier. The time constant of the external circuit has to be kept small compared with the charge collection time, so that the current flowing through the load resistance is essentially equal to the instantaneous value of the current flowing in the detector. For this purpose, the signal is read out from the back side of the device so that the implant strip resistance (that is of the order of 1 MΩ) does not affect the time constant of the readout. The load resistance has been chosen to be 10 Ω that is the best compromise between two conflicting needs: a low time constant and a good current injection in the charge amplifier. In order to prevent the introduction of additional, not controlled, parasitic series resistance to the load resistance, the sensor's backplane will be wire-bonded to the readout circuit, rather than being connected using a conductive glue. This adopted solution has lead to a significative improvement in terms of time response and uniformity of signal waveform among the seven silicon sensors. A multiple stage cascade amplifier configuration has been chosen, both for the single sensor readout as well for the sum circuit, in order to increase the gain bandwidth up to 300 MHz.

Figure 6 (left) shows the digitized readout signal as a function of time, both from a single channel and from the analog sum output, obtained by iniecting a fast (~ 2ns) pulse in the electronics. The vertical dashed lines indicate the 16 ns time separation between two consecutive pulses. The very fast response guarantees that the electronics does not affect the time response of our devices. Figure 6 (right) shows the corresponding electronic noise, proving that an excellent signal to noise ratio is achieved. The slight differences between the single channel and the analog sum, in the signal gain and noise, are due to the additional stage of amplification included in the analog sum circuit, as shown in figure 5 (right).

2017 JINST 12 C02051

Table 2. Main parameters of the PicoQuant LDH-P-1060 laser used to test silicon devices.

Light Wavelength	1060 nm
Repetition Rate	up to 80 MHz
Pulse FWHM	< 100 ps
Max Average Power	21 mW

6 The gamma calorimeter: test results on a first prototype

A pulse of laser light focussed on a semiconductor can induce a localized transient generation of electron-hole pairs, if the photon energy is greater than the semiconductor band gap energy. As a result, it can mimic the signal induced by ionizing particles and be used for testing purposes.

The time response of the first prototype of the front end board equipped with seven silicon detectors (see figure 5) has been measured using a PicoQuant (mod. LDH-P-1060) pulsed laser diode whose characteristics are reported in table 2. A laser wavelength of 1060 nm, which corresponds to a penetration depth of 900 μm in silicon, well above the sensor thickness, has been chosen in order to guarantee a uniform energy deposition along the whole depth of our devices. The laser pulse lasts less than 100 ps, so it is short enough compared to the charge collection times of a 300 μm thick silicon device that is of the order of a few ns; we are therefore confident that the detector signal is not distorted by the duration of the pulse. The high value of the average power allows simulating very large energy depositions as the ones expected at the ELI-NP facility. Furthermore the large rate of emitted light pulses gives us the possibility to reproduce the same temporal structure of the ELI-NP gamma beam using an external trigger and burst mode operation.

The data acquisition is based on a CAEN Switched Capacitor Digitizer (mod. V1742 [7]) that is able to sample the analog input signals in a circular memory buffer made of 1024 cells at a selectable sampling rate from 1 to 5 GHz. As a trigger signal arrives, all the analog memory buffers are frozen and digitized with a resolution of 12 bits into a digital memory buffer with independent read and write access. We plan to operate the digitizer at a sampling rate of 1 GHz, during the real data acquisition, in order to acquire the whole macro-bunch. A higher frequency is used for a better characterization of the signal profile during the ongoing phase of fine tuning of the electronic parameters. In figure 7 (left) the device response to a single laser pulse is shown. Despite the fast response of the front end electronics, after 16 ns from the peak time the signal is not back to the zero line; this generates a signal pile-up that amounts to about 1% contribution, due to the signal coming from the previous pulse. Figure 7 (right) represents the front end response to a train made of 32 laser pulses. By comparing several events, we observe a reproducible structure in the series of single pulse height. The more evident effect is on the first pulse that is always a few per cent higher than the following ones. Using a calibrated fast photodiode we verified that this particular structure is a feature of the emission intensity of our laser, when operated in burst mode, and it is not ascribable neither to our sensors nor to the readout electronics. The red line represents the result of a fit algorithm based on single pulse deconvolution. The measured single pulse response is used as a template function and the fit function is computed as the sum of 32 template functions, shifted by 16 ns and weighted with a fit parameter representing the height of the single pulse. The fit results

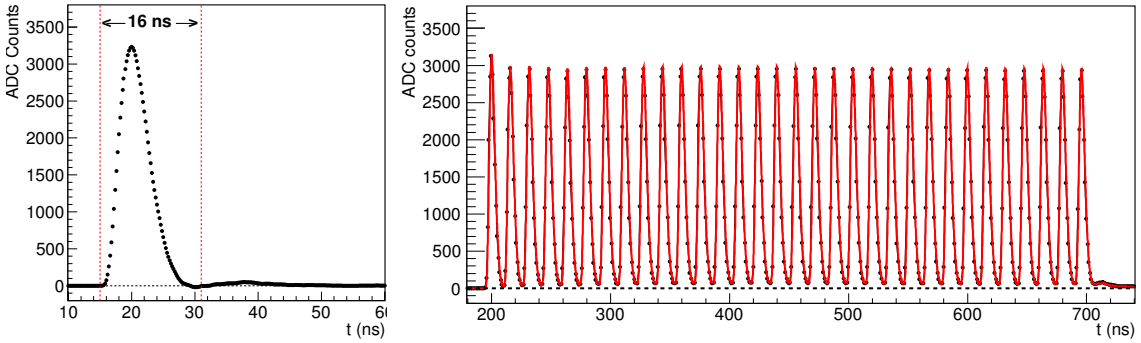

Figure 7. Left: sensor response to a single laser pulse. Right: sensor response to 32 laser pulses separated by 16 ns.

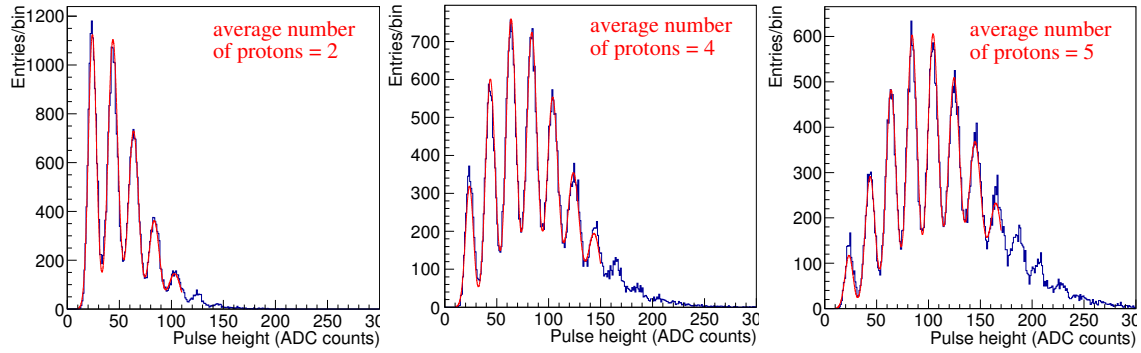

Figure 8. Acquired spectra for different average multiplicities (2, 4 and 5, respectively) of proton per pulse.

have been validated using simulated events. The procedure has proven the capability of detecting differences in amplitude of the order of per mil among single pulses. In addition, the good agreement between the fit function and the detector response demonstrates that the charge pile-up, due to the high pulse rate, does not degrade the signal waveform. This makes us confident that our silicon sensors, equipped with custom fast electronics, will be able to disentangle pulses separated by 16 ns and measure the pulse height with an accuracy at the level of per mil, allowing the calorimeter to measure the beam energy and intensity and their variation in time within a ELI macro-pulse.

An absolute energy calibration procedure of the silicon device equipped with custom electronics has been evaluated by exposing the first prototype of the readout board to a pulsed proton beam at the Labec facility, in Florence [8]. The chosen proton energy was 3 MeV and the average number of impinging protons was modified during data taking. Since the range of such protons in silicon is less than 100 μm, we expect the proton energy to be fully deposited in our devices. Figure 8 shows the acquired spectra for different average multiplicities of particles per pulse. The solid line represents a fit to experimental data obtained using a Poisson distribution convoluted with a sum of Gaussian distributions. The peaks are equally spaced at integer multiples of the proton energy; therefore the distance between consecutive peaks provides an absolute energy calibration for our devices. In addition, increasing the average value of the proton multiplicity distribution, we can simultaneously

2017 JINST 12 C02051

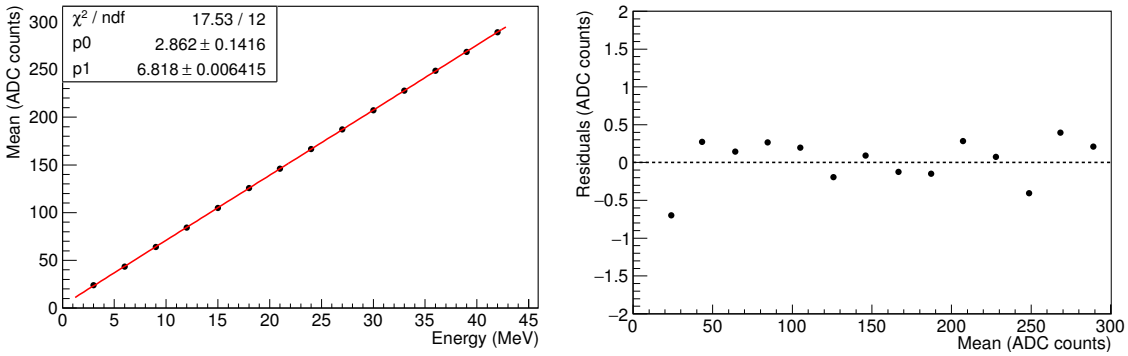

Figure 9. Linearity results (left) and fit residuals (right) for silicon sensors equipped with custom electronics tested with a proton beam.

detect events with a largely variable number of particles per pulse and thus verify the linearity of the signal response by plotting the mean value of the Gaussian peaks as a function of the known deposited energy, as shown in figure 9 (left). Once the final version of the front end electronics will be ready, we plan to repeat the linearity measurement up to larger energy depositions, similar to the ones expected at the ELI-NP facility. On the right side of figure 9, the residuals, which are computed as the deviations from the best linear fit, are reported as a function of the measured energy in ADC counts. The linearity accuracy turns out to be of the order of a few per mil.

7 Conclusions

A characterization system, composed of four specifically designed detectors, is currently being developed in order to measure and monitor the unprecedented characteristics of the gamma beam that will be delivered at the ELI-NP facility, in Romania. In particular, a new concept gamma calorimeter has been designed to measure the average energy and intensity of the beam. The detector will be made of 22 blocks of polyethylene absorber interleaved by active silicon layers. Since the photon interaction cross section in the low-Z absorber strongly depends on the energy of the impinging photons, the average beam energy can be reconstructed by the longitudinal profile of the energy deposition. The number of incident photons can then be inferred from the total energy released thanks to the narrow energy bandwidth of the beam. Accurate Monte Carlo simulations indicate that the statistical accuracy on the average beam energy and on the number of photons is expected to be better than one per mil after a few seconds of operation. Tests on prototype boards show that silicon sensors equipped with fast custom readout electronics are able to disentangle pulses separated by 16 ns with an accuracy at the level of per mil. The feasibility of an absolute energy calibration has been evaluated by exposing a prototype to a proton beam; this test has also proven the linearity of the detector response with respect to the deposited energy with an accuracy of the level of per mil. We are therefore confident that this device will be able to measure beam energy and intensity and their variation within a macro-pulse with an accuracy at the level of a few per mil.

2017 JINST 12 C02051

References

[1] O. Adriani et al., *Technical design report EuroGammaS proposal for the ELI-NP gamma beam system*, arXiv:1407.3669.

[2] C.A. Ur et al., *The ELI-NP facility for nuclear physics*, *Nucl. Instrum. Meth.* **B 355** (2015) 198.

[3] P. Cardarelli et al., *Monte Carlo simulation of a collimation system for low-energy beamline of ELI-NP gamma beam system*, *Nucl. Instrum. Meth.* **B 355** (2015) 237.

[4] M.G. Pellegriti et al., *EuroGammaS gamma characterisation system for ELI-NP-GBS: the nuclear resonance scattering technique*, *Nucl. Instrum. Meth.* **A** (2016) in press.

[5] L. Borrello et al., *Sensor design for the CMS silicon strip tracker*, CMS-NOTE-2003-020, CERN, Geneva Switzerland, (2003).

[6] GEANT4 collaboration, S. Agostinelli et al., *GEANT4: a simulation toolkit*, *Nucl. Instrum. Meth.* **A 506** (2003) 250.

[7] CAEN, *V*1742 *technical information manual*, http://www.caen.it.

[8] N. Taccetti at al., *The pulsed beam facility at the* 3 *MV Van de Graaff accelerator in Florence: overview and examples of applications*, *Nucl. Instrum. Meth.* **B 188** (2002) 255.

2017 JINST 12 C02051